RSC Advances

PAPER

View Article Online
View Journal | View Issue

Cite this: *RSC Adv.*, 2025, **15**, 12321

Opto-sensing of sotalol using parafilm and poly(methyl methacrylate) micro-plates decorated by silver nanoparticles: state-of-the-art for one-drop pharmaceutical analysis†

Milad Baghal Behyar,[a] Farnaz Bahavarnia,[b] Azadeh Nilghaz,[c] Mohammad Hasanzadeh *[d] and Nasrin Shadjou [e]

Sotalol is an antiarrhythmic drug with a narrow therapeutic index and potential adverse effects, including hypotension and heart block, requiring continuous and precise blood-level monitoring. In this study, an innovative optical sensor was developed using silver nanoparticle (AgNP)-functionalized parafilm (PF)- and poly methyl methacrylate (PMMA) for the trace-level detection of sotalol in human blood plasma. The detection was performed using CMYK-based colorimetric digital image analysis *via* the Color Picker software app, achieving a low limit of quantification of 1 μM and a linear range of 0.001 to 20 mM. The selectivity of the sensor was also validated in the presence of potentially interfering cardiovascular drugs. Nanoparticle characterization revealed a shift in zeta potential (Z_p) from −14.5 to −6.16 mV, confirming a strong interaction between sotalol and AgNPs, as the optical probe. The sensor offers an innovative, cost-effective, portable, and rapid (5-min analysis time) approach for detecting sotalol in blood plasma. This sensor holds significant potential for point-of-care diagnostics and *on-site* drug monitoring, providing a reliable alternative to conventional, lab-dependent analytical methods for therapeutic drug monitoring.

Received 10th March 2025
Accepted 13th April 2025

DOI: 10.1039/d5ra01716e

rsc.li/rsc-advances

1. Introduction

Sotalol is a non-selective beta-adrenergic blocker exhibiting class III antiarrhythmic effects. It is commonly prescribed for managing atrial fibrillation and controlling recurrent ventricular arrhythmias.[1] Developing robust analytical techniques for the detection of sotalol in blood is crucial.[2] Chromatographic methods are commonly used to detect β-blockers.[2–5] Electrochemical sensors of β-blockers as sensitive methods that do not normally require a pretreatment process have gained importance due to their reliability, high specificity and rapid response. These methods have not required time-consuming preparation methods, the use of expensive and dangerous solvents, and the need for professionals.[6–8] But, reliability is one of the main limitations of these methods. Therefore, there is a need to develop a simple, rapid, and low-cost method to determine sotalol in blood.

Colorimetric techniques have emerged as effective and economical methods for detection of drugs in real samples. In particular, research methods based on colorimetric sensing by nanoparticles (NPs) as the optical probe, have become widespread due to their high sensitivity.[9,10] Therefore, traditional NP-based colorimetric analysis is commonly conducted using conventional plates in a plate reader, which are inconveniently stationary and rely on the sample volume.[11]

The incorporation of NP-based sensors into microfluidic devices presents a challenge in the development of colorimetric sensors, despite their advantages of low cost, speed, ease of fabrication, small sample volume requirement, and portability.[11,12] The use of novel technologies in analytics has become widespread in recent years. This includes recording and processing digital images to identify and eliminate expensive devices. Digital imaging techniques are particularly attractive for use in colorimetric sensors, as they can cause electrical reactions when the color molecule reactant material is visible light[13,14] Detection of analyte's color in computer vision is carried out in the form of color recognition. The yellow detection method was developed with a paraffin film substrate and a PMMA panel. This converts RGB colors to another desired

[a]*Nutrition Research Center, Tabriz University of Medical Sciences, Tabriz, Iran*
[b]*Asian Nano Ink Science Based Company, Tabriz University of Medical Sciences, Tabriz, Iran*
[c]*Drug Delivery, Disposition and Dynamics, Monash Institute of Pharmaceutical Sciences, Monash University, Parkville, VIC 3052, Australia*
[d]*Pharmaceutical Analysis Research Center, Tabriz University of Medical Sciences, Tabriz, Iran. E-mail: hasanzadehm@tbzmed.ac.ir*
[e]*Department of Nanotechnology, Faculty of Science and Chemistry, Urmia University, Urmia, Iran*

† Electronic supplementary information (ESI) available. See DOI: https://doi.org/10.1039/d5ra01716e

color space,[15] namely cyan magenta (CMYK) color spaces.[16,17] The yellow lines in the CMYK color model are used to distinguish yellow from the background. Normal yellow can be easily detected in colored medium, but dark yellow is often overlooked in practice.[18,19] This study presents an innovative yet straightforward colorimetric method for detecting and quantifying sotalol in human samples utilizing AgNPs. Results can be visually proven using UV visual spectroscopy or using a PF/PMMA-based colorimetric device (PCD) to determine the amount of sotalol in the actual sample. μPCDs are formed by using heat to transfer the microfluidic structure of paraffin-coated substrate to a clean fiber optic blade. The device then uses AgNPs to quickly and easily recognize sotalol in blood samples. There are many ways to generate sensor data, one of the most popular is the colorimetric analysis method.

Wax was selected as a key material because of its broad availability and eco-friendliness. Wax screen printing is highlighted as a cost-effective means of creating PCDs using common wax printers and affordable printing paper. The process involves printing wax patterns onto paper using simple techniques and eliminates the need for sterilization, UV exposure, organic solvents, or intricate materials. Furthermore, its scalability enables the method to be used with hot plates or equivalent facilities, a significant advantage in producing μPCDs in resource-limited regions. Point-of-care diagnostic devices (PCDs) are gaining recognition as low-cost, user-centric, disposable, and non-invasive tools poised to make a transformative impact on global healthcare, aiding in disease diagnosis and treatment, particularly in disadvantaged or medically underserved areas. In light of existing methods for detecting sotalol in body fluids, which often suffer from issues like low sensitivity, lack of specificity, and cumbersome procedures, this new study introduces silver nanoparticles (AgNPs) as highly effective optical nanoprobes for detecting sotalol in human plasma.[11] Here, AgNPs with prism morphology were employed for the first time to detect sotalol in real samples. The sensor enables direct quantification in chemical samples without necessitating derivatization or sample preparation processes. Thanks to the simplicity and portability of OD-PCD, it holds significant potential as an efficient tool for monitoring and tracking applications. This technique is anticipated to improve environmental health and workplace safety, while also advancing colorimetric analysis by enabling the sensitive and selective detection of sotalol. It provides a versatile platform for analyzing not only sotalol but also other β-blockers. To the best of our knowledge, no prior studies have been reported on the colorimetric sensing of sotalol using PCD-based analysis. Moreover, the utilization of PCD decorated with AgNPs for sotalol detection is novel, effectively precluding a comparative analysis of nanoprobes currently available. Using engineered colorimetric sensing platform, sotalol was recognized in human real samples by CMYK color analysis and related app installed in smartphone-captured digital images. Obtained results allowing PCD to be effectively applied for sotalol quantification. This work pioneers the use of AgNPs with exceptional stability and excellent optical properties, acting as a reagent-free optical sensing probe, in tandem with optimized PCDs for the recognition of sotalol. Furthermore, it introduces a novel time and

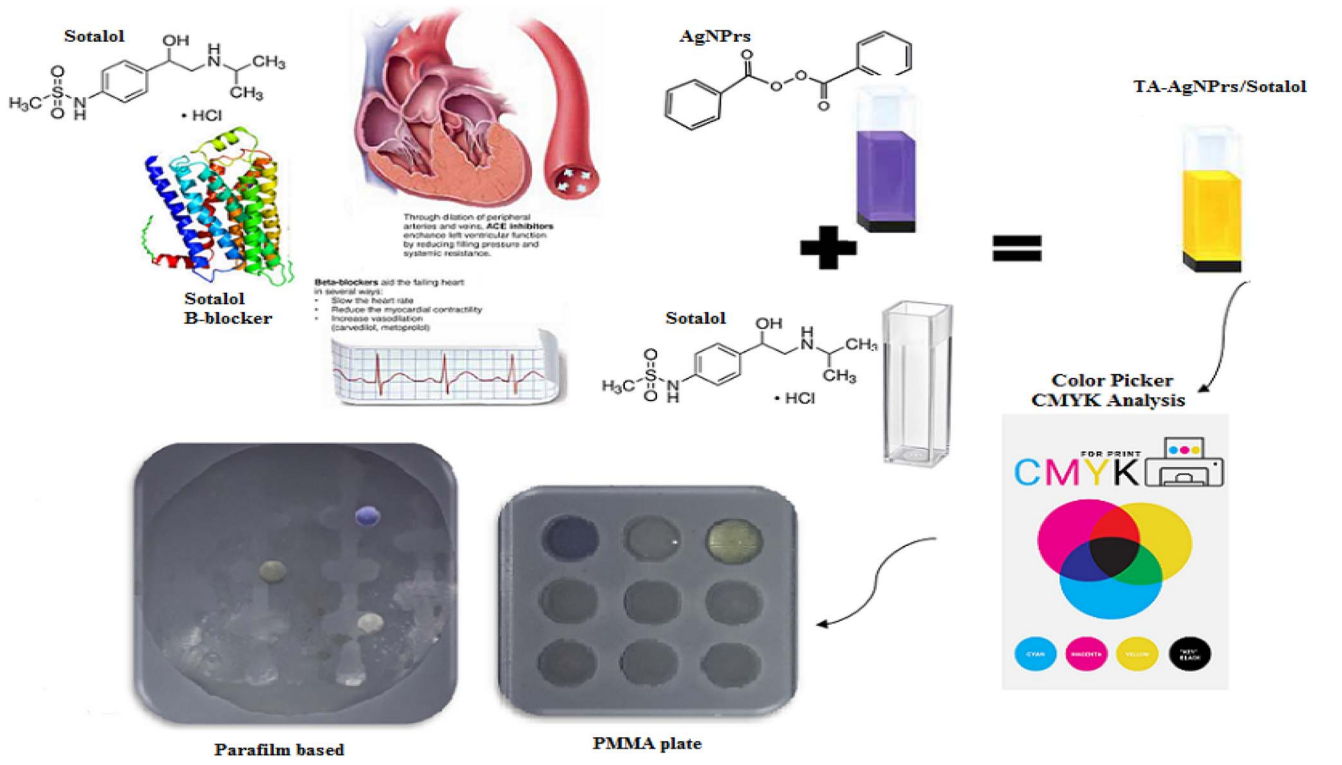

Scheme 1 Schematic illustration of sotalol detection using AgNPs as an optical probe, analyzed *via* CMYK-based colorimetric detection.

color-based semi-analytical recognition approach. Scheme 1 outlines the overall procedure for the chemical recognition of sotalol enabled by the AgNPs optical sensor system.

2. Experimental

2.1. Reagents and materials

Sotalol, famotidine, indomethacin, diazepam, mefenamic acid, ibuprofen, dapoxetine, codeine, and pantoprazole were purchased from Sobhan Darou Company. Silver chloride (AgCl), silver nitrate ($AgNO_3$), sodium borohydride ($NaBH_4$, 96%), trisodium citrate ($Na_3C_6H_5O_7$), hydrogen peroxide (H_2O_2, 30 wt%), polyvinylpyrrolidone (PVP) K-30, and acetonitrile were obtained from Sigma-Aldrich, Canada. Deionized water was supplied by Ghazi Pharmaceutical Company, Tabriz, Iran, and PF sheets were received from Temad-Kala, Tehran, Iran.

2.2. Instrument

The analysis of size distribution and zeta potential for the synthesized AgNPs was carried out using a Malvern Instruments DLS/ZETA potential analyzer from England, with reference code MAL1032660 (size range: 0.3 nm to15 μm, minimum sample volume: 3 μL, temperature range 0 to 90 °C). The successful synthesis of AgNPs was verified through transmission electron microscopy (TEM) performed in Adelaide, Australia, at an accelerating voltage of 200 kV. Detailed imaging of the NP surface was achieved *via* field-emission scanning electron microscopy (FE-SEM; Hitachi-Su8020, Czech Republic) operating at a voltage of 3 kV. Spectroscopic properties were assessed using a Shimadzu UV-1800 UV-vis spectrophotometer. Furthermore, all images and videos included in this research were captured using a Samsung Galaxy A5 smartphone equipped with a 13-MP camera, autofocus enabled, and supplemented by the free Color Picker app installed on the smartphone.

2.3. Synthesis and characterization of AgNPs

AgNPs were synthesized and characterized according to our previous reports.[11,20–24]

2.4. Real sample preparation

Human blood plasma samples were supplied by the Iranian Blood Transfusion Research Center, operating under IRCT-Tabriz, Iran. The samples were processed by centrifuging with acetonitrile (1 : 1 v/v) at 8000 rpm for 10 min. The resulting supernatant was transferred to a 2 mL vial for subsequent colorimetric and spectrophotometric analyses.

2.5. Fabrication of PF-based PCDs

This study underlines the innovative application of PF in crafting hydrophilic channels for droplet deposition to advance colorimetric analysis. PF, a flexible and semi-transparent thermoplastic polymer, was placed as an interposing layer between an iron mold and a magnet, enabling paraffin to penetrate the PF's structure and form hydrophilic channels on its surface. This process facilitates substrate infiltration, creating hydrophilic layers that are well-suited for efficient diagnostic applications.

The material becomes liquefied at a temperature of 90 °C, followed by a 30-second immersion of the relevant substrate. Once dried, the iron mold undergoes heating at 85 °C for 10 seconds. A layer of PF is again interleaved between the mold and the magnet, promoting the formation of hydrophilic channels as paraffin saturates the PF's structure. The resulting hydrophilic region is designed in a cluster of 28 circles as the reaction zone. A digital design drafted using Corel DRAW software was employed to produce a metal stencil tailored with precise dimensions. After drying, PCDs were utilized for colorimetric analysis.

The PCDs were fabricated with a geometric arrangement of 28 circular recognition zones designed for microfluidic functionality. The configuration includes a central circular zone (5 mm in diameter) connected to 28 surrounding detection zones (12 mm in diameter) *via* internal channels measuring 3 mm in width and 9 mm in length. The final dimensions of the PCDs stood at 50 mm × 50 mm. These PF-based PCDs were effectively applied to detect sotalol by leveraging optical nanoprobes (AgNPs). This method shows strong promise for developing rapid, low-cost sotalol diagnostic kits with improved qualitative performance, facilitated by the paraffin-induced modification of PF's surface properties (Fig. S1 and Video in ESI†).

2.6. PMMA plate fabrication

The RDWorkV7 software was utilized to design the layout of 5 mm diameter and 1 mm depth wells. This design was then transferred onto a 2 mm thick PMMA plate using a CNC laser cutter. The wells were created by configuring the laser to operate at a speed of 15 and a power of 15.5. To separate the outline from the plexiglass, the final cutting step was executed by setting the laser (Fig. S2†).

3. Results and discussion

3.1. Detection of sotalol by colorimetric and spectrophotometric (UV-vis)

The AgNPs solution exhibited a navy-blue color with a UV-vis spectrophotometric absorption peak at 436 nm and emission in the range of 200 to 800 nm. The UV-visible spectrum showed that AgNPs have an absorption peak at about 336, 437, and 581 nm. After interacting AgNPs with sotalol, the color of the solution turns yellow. Then, colorimetric and UV-vis spectrophotometry methods can be utilized for opto-sensing of sotalol (Fig. 1). The UV-vis spectra of the AgNPs show broad features with three distinct bands located at 336, 437, and 581 nm. Upon the addition of sotalol. Interestingly, after 30 min of reaction, this peak was moved to 429 nm which confirmed the successful interaction of the optical probe with the analyte sample (Fig. 1). These observations highlight that the detection of sotalol using the AgNPs is strongly influenced by the nanoprism shape in relation to the position of the in-plane dipole resonance peak.

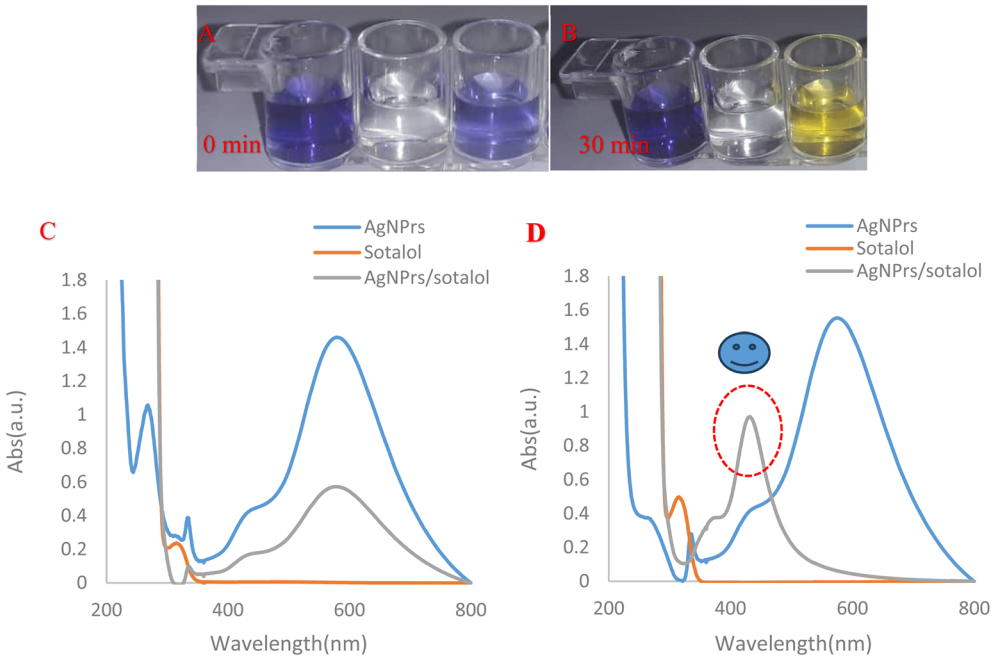

Fig. 1 (A and B) Colorimetric images of (1) AgNPs (2) sotalol (10 mM) (3) AgNPs/sotalol (10 mM). (C and D) UV-vis of AgNPs, sotalol (10 mM), and AgNPs/sotalol (10 mM) in 0, 30 min incubation of optical probe with analyte.

Based on colorimetric results, the AgNPs (optical probe) solution exhibited a navy-blue color with a spectrophotometric absorption peak at 436 nm. In addition, AgNPs exhibited UV/visible absorbtion peaks in the range of 300 to 600 nm. Due to the interaction of optical prob with sotalol, the color of the solution turns yellow. Also, introducing sotalol to the optical probe solution leads to the accumulation of more AgNPs, causing a color change. Based on obtained results, sotalol has basic functional groups (an amine group, NH_2) that can interact with the negative surface charge of AgNPs *via* electrostatic attraction. Amines (NH_2) are often protonated at physiological pH, forming positively charged NH_3^+ groups. The AgNPs are stabilized with anionic ligands such as citrate or chloride. So, the positively charged amine of sotalol would be attracted to AgNPs surface with nanoprism structure.

The AgNPs could interact with sotalol molecules, altering their optical properties, stability, and electronic properties due to the adsorption of the drug. These results support the potential of AgNPs for effective sotalol detection, the strongest peaks at 436 nm for AgNPs/sotalol appeared after 30 min, as shown in Fig. 1. These results were confirmed by DLS/zeta analysis of the probe after its reaction with the sotalol (Fig. S3†). The strongest peak was appeared at 436 nm after 30 min, as shown in Fig. 1. DLS/zeta potential was utilized to study the interaction of AgNPs with sotalol. DLS results showed that the average particle size of AgNPs was 41.38 nm (Fig. S3†). Interestingly, after the interaction of AgNPs with sotalol, the average size of the optical probe particle decreases to 33.10 nm which illustrate successful interaction of optical probe with the candidate analyte (sotalol). The reaction of sotalol with AgNPs can involve several possible interactions depending on the conditions (pH, forming positively charged NH_3^+ groups, an amine group, NH_2, reducing agents, and stabilizers). Below are some potential reaction pathways binding, surface modification, charge transfer, hydrogen bonding, and π–π stacking. The binding of sotalol with AgNPs might change its solubility. So, morphology of AgNPs could potentially alter. Therefore, its optical properties could be changed. On the other hand, AgNPs could become coated (interacted) with sotalol, which might alter their optical properties, stability, and electronic properties due to the adsorption of the drug. Importantly, electrostatic interactions may also facilitate electron transfer between the AgNPs and sotalol, potentially changing the redox state of either the drug or the nanoprisms, though this would be less likely unless specific conditions (like light or pH shifts) are applied. Interestingly, the hydroxyl group on sotalol can engage in hydrogen bonding with the surface atoms of the AgNPs. This can contribute to stabilizing the biding of sotalol to the nanoparticles. Finally, the benzene ring in sotalol could also interact with the nanoprisms *via* π–π stacking if there are sufficient aromatic interactions between the surface of the nanoprisms and the aromatic ring of sotalol. This would be a non-electrostatic interaction but could add to the overall binding strength.

For more confirmation of obtained results by spectrophotometry and DLS/Zp, the TEM images were recorded in two reaction conditions before and after incubation of optical probe with analyte (sotalol). As can be seen in Fig. S5 and S6,† morphology of AgNPrs were charged significantly to tubular structure.

3.2. Analytical study

This study used both colorimetric and spectroscopy methods to investigate the interaction of sotalol with AgNPs. Sotalol with concentrations ranging from 1 μM to 20 mM were prepared, and AgNPs were added in equal volumes. The results show that the

effect of sotalol on AgNPs is influenced by both its concentration and duration of the analyte with an optical probe, there is no reaction between them. Interestingly, after 5 min, only the color of the first concentration of sotalol (20 mM) was changed to dark yellow. Importantly, for the concentration of 6–20 mM, the color of the reaction was changed to yellow after 30 min when the sensing process was completed. At the low concentration of analyte from 1 μM to 6 mM, the sensing process was completed after 60 min. This result is related to kinetic of reaction and analyte concentration (two main effective factors

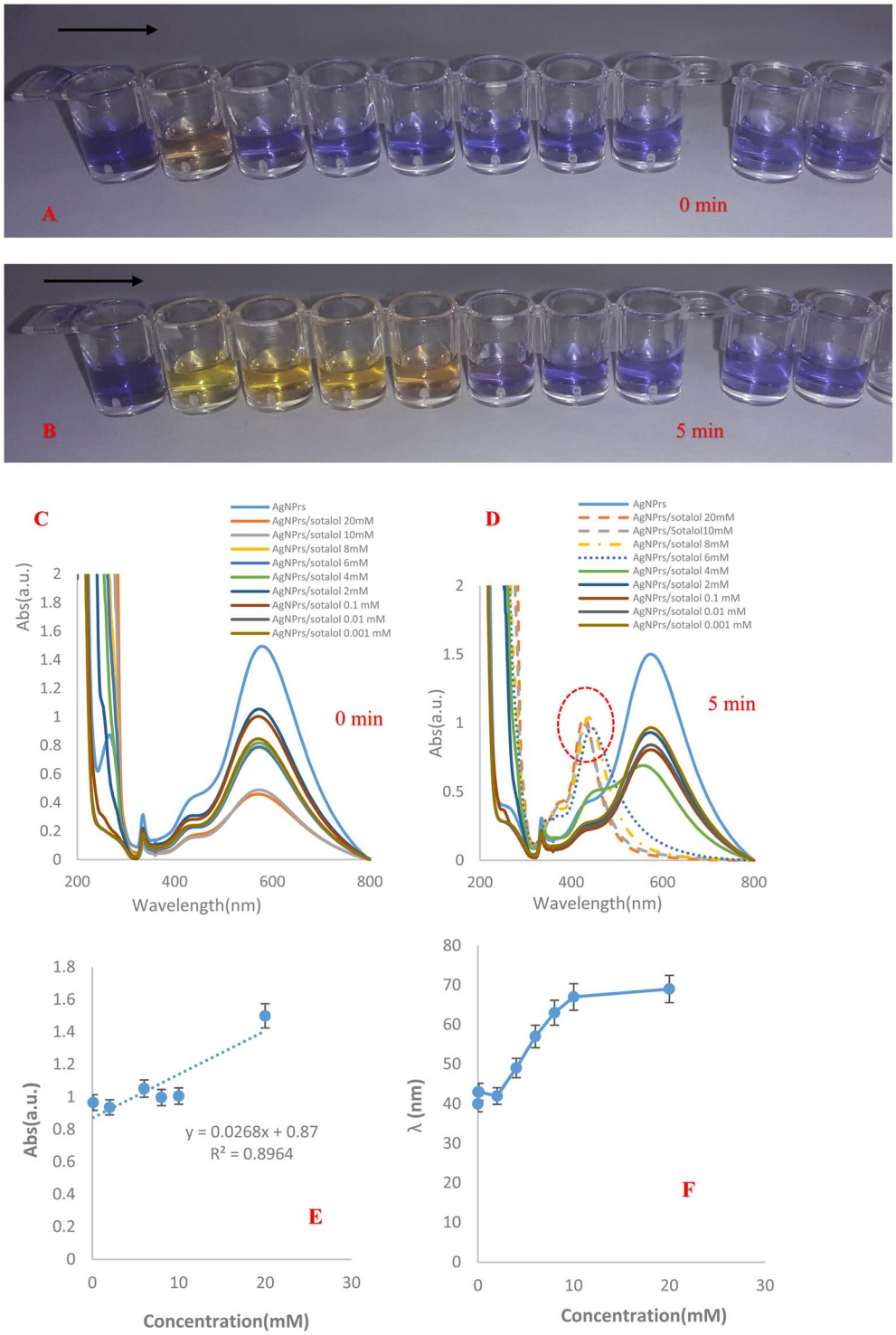

Fig. 2 (A and B) Colorimetric images of AgNPs and AgNPs/sotalol in different concentrations (0.001, 0.01, 2, 4, 6, 8, 10, 20 mM) in two incubation times of 0 and 30 min. (C and D) UV-vis spectra of AgNPs, AgNPs/sotalol in different concentrations (0.001, 0.01, 2, 4, 6, 8, 10, 20 mM) in 5 min of incubation time (E) calibration curve of colorimetric sensor in 30 min of incubation time (F). Variation of λ (nm) of optosensor *versus* concentration of sotalol in 5 min of incubation time.

on the above-mentioned sensing mechanism). Therefore, the concentration of sotalol has significantly affect on the colorimetric sensing mechanism of this drug by the proposed optical prob (AgNPs) that utilized in the structure of the engineered platform. The results were also confirmed by UV-vis spectrophotometry analysis. According to UV-vis spectra, for the concentration range of 6, 8, 10, 20 mM, wavelength of UV-vis spectra peak of the optical probe (587 nm) shift to 433, 437, 442, 447 nm, respectively. A calibration curve was obtained using digital image analysis by the processing of CMYK obtained from digital photography by smartphone camera. The Color-Picker image processing toolbox was utilized to capture wavelengths and their associated CMYK values. The color intensity was subsequently converted into absorbance values using the Beer–Lambert equation (Table S1†). Fig. 2E demonstrates the use of digital image analysis and the plotting of calibration curves for sotalol based on the CMYK digital color analysis which detected by smartphone cameras. CMYK data further corroborate this observation, displaying an alignment with the yellow color range as evidenced by the correlation: The *Y* (Yellow) plot exhibits the highest R^2 value, reflecting a significant slope and pronounced linearity as Abs (a.u.) = $0.0268C_{\text{Sotalol}} + 0.087$, $R^2 = 0.8964$ (incubation time of 30 min), with a low limit of quantification (LLOQ) of 1 μM. These findings establish a significant relationship between the absorbance data obtained from the calibration curve and the analyte concentration. In addition, if we draw variation of wavelength *versus* concentration of analyte, it is show that, wavelength of optical probe (587 nm) decreased significantly. The obtained graph indicates a downward trend where rising concentrations of sotalol result in increased wavelength values, with higher concentrations gravitating toward the yellow wavelength spectrum.

The proposed colorimetric platform addresses a critical need for accessible analytical tools in pharmaceutical quality con strategy, this study aims to provide a practical solution for sotalol analysis that can be deployed in resource-limited settings or POC applications.

3.3. Colorimetric analysis using one-drop PF- and PMMA-based PCDs

Using a PF or PMMA plate, we developed two types test devices to investigate PCD-based recognition system for sensing sotalol. The system uses wax foam technology to eliminate the need for special device conditions. To integrate the calorimetric sotalol analysis system into PF and PMMA plates of PCD, combined with a 1 : 1 v/v ratio with an AgNPs probe solution with a 1 : 1 v/v ratio with concentration of 10 μL, 10 μL, the color alteration rapidly begins, and the AgNPs demonstrate a discernible change after 30 min (Fig. 3A–D and V S1†), The color transitioned from blue to yellow, becoming distinctly yellow after 30 min.

We developed PCD-method tools for the colorimetric analysis of sotalol using portable sensing which is simple, cost-efficient, and adaptable design. For this purpose, we use

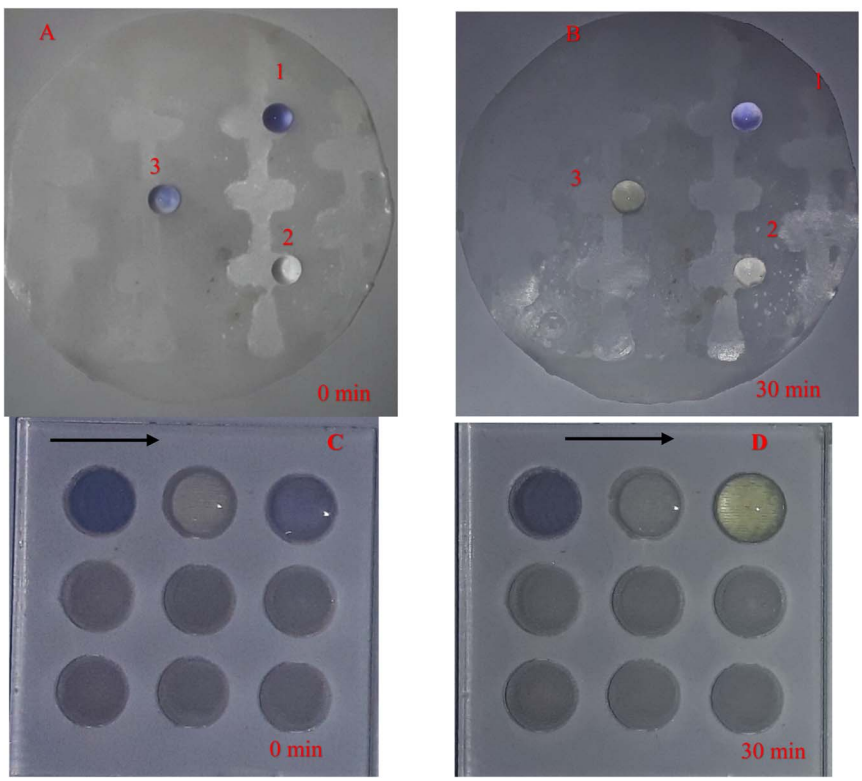

Fig. 3 (A–D). Colorimetric detection of sotalol using PF and PMMA-based PCDs for (1) AgNPs (2) sotalol (10 mM) (3) AgNPs/sotalol (10 mM) in two incubation times of 0 and 30 min, respectively.

parafilm as suitable substrate. Parafilm, a thin and transparent sheet classified as a flexible thermoplastic polymer, serves as a key material in this setup. It remains stable under both hot and cold conditions and, even when melted, retains its chemical composition. Upon cooling, it reverts to its original form. It does not decompose at high temperatures; instead, it only experiences changes in shape, structure, or state. The system is structured into 28 distinct zones, each designed for a specific sample analysis. For testing, 10 μL of AgNPs was first applied to each visible area, followed by another 10 μL of the analytical solution. Zone 1a was specifically assigned to AgNPs. From Zone 2 onwards, various sotalol concentrations, ranging from 1 μM to 20 mM, were applied (Fig. 4A1 and A2, and V S2†). Zones exposed to higher sotalol concentrations underwent rapid color

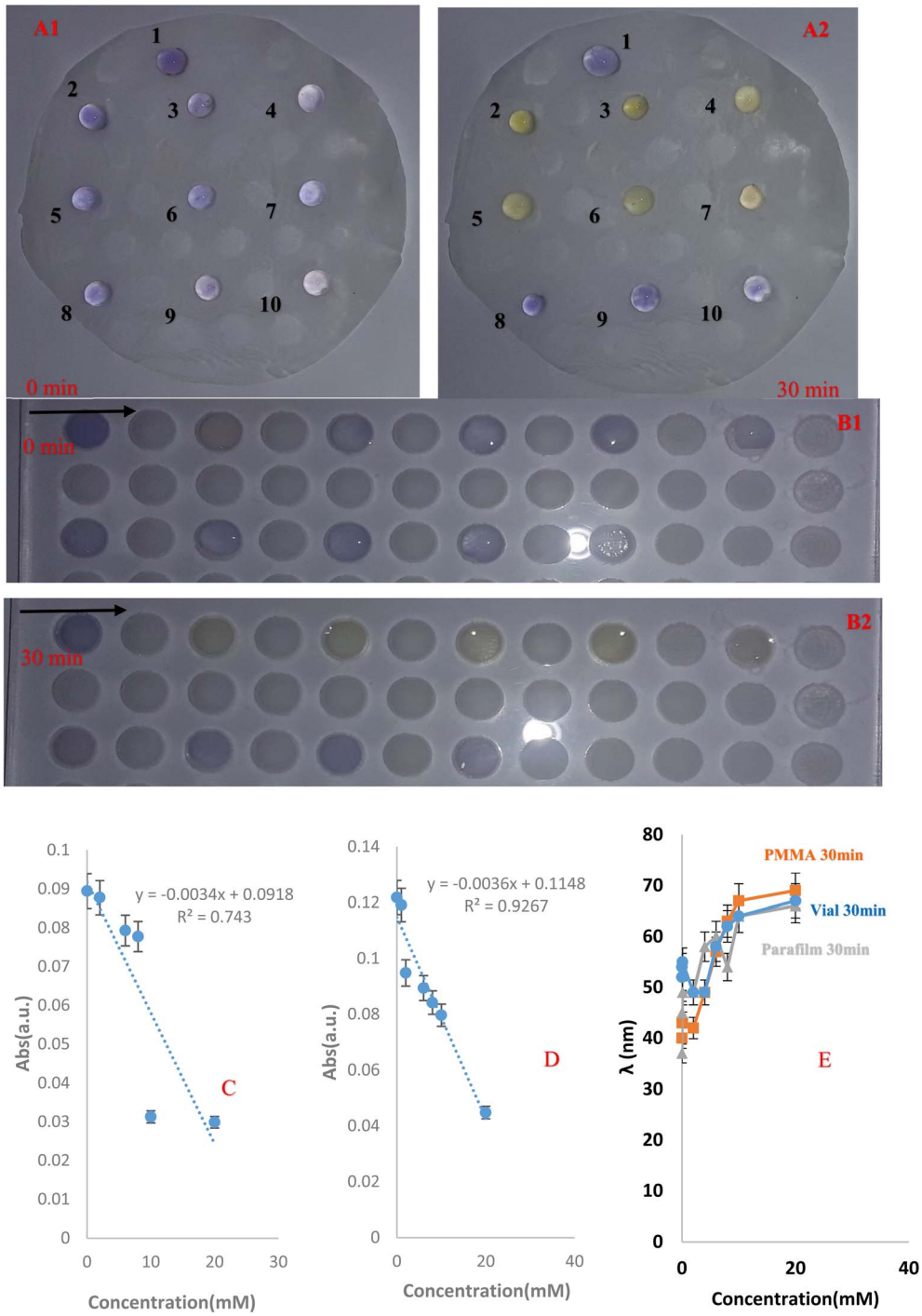

Fig. 4 Colorimetric determination of sotalol (0.001, 0.01, 0.1, 2, 4, 6, 8, 10, and 20 mM) using engineered colorimetric platform using PF (A1 and A2)- and PMMA (B1 and B2)-based PCDs decorated by optical prob (AgNPs). (C and D) Calibration curves using PF- and PMMA-based PCDs, respectively. (E) Sigmoid plot based on dependency of λ (nm) of opto-sensor *versus* concentration of analyte.

transformations compared to others, with visible changes noted 30 min after testing (Fig. 4B1 and B2). As the incubation period progressed, the entire sotalol concentration spectrum exhibited a complete transition to yellow. Notably, high concentrations applied on PMMA plates yielded results identical to those observed on the parafilm substrate, as demonstrated in Fig. 4(C and D). Correlation coefficient values from linear analysis were found to be 0.9217 for the PF substrate and 0.9041 for the PMMA plate. The noticeable color changes were visually examined, while the Color Picker software further validated the efficient mobility of PCD, facilitating robust detection of sotalol in real samples. The absorption rates of the analyte samples were analyzed following Beer–Lambert law. As described by this optical law, the light absorption by different solution layers remains consistent, regardless of the emitted light's intensity. Together, Beer and Lambert's laws establish a direct linear relationship between the concentration of a solution and the light it absorbs. Specifically, Lambert's law states that the quantity of light absorbed by a solution is constant, irrespective of the intensity of the light source.[25] This experiment incorporates a smartphone application called the Color Picker Analyzer, which functions as a light detector by instantly calculating the average CMYK values of images captured in real-time through the camera's view. The investigation uses light either reflected from a parafilm layer or emitted from a computer monitor as the light source. A loss (OD) approach was applied in the chemical analysis of sotalol, aimed at reducing the consumption of both analytes and solvents during the monitoring process.[26]

As a result, a compact and efficient kit was developed for the determination of sotalol concentrations, achieving a LLOQ of 1 μM. The interaction between sotalol and AgNPs based on interaction was evaluated *via* a visible color change observable within 30 min. Subsequently, a sigmoid curve was plotted by correlating λ (nm) with sotalol concentrations (Fig. 4E), confirming the wavelength shifts corresponding to changes in analyte concentrations. Furthermore, as visualized in the colorimetric data graphs, an increase in the *Y*-value corresponds to a reduced bending radius. This approach highlights the innovative use of the parafilm substrate in this study, considered a notable advancement compared to the conventional PMMA substrate and glass vials (refer to Tables S2–S4 in the ESI†).

The analytical performances of various methods for sotalol detection, such as UV-vis and fluorescence, surface-enhanced Raman scattering (SERS) and electrochemical sensors, voltammetric method, and high-performance liquid chromatography (HPLC), were compared with the method developed in this study. Most of the reported techniques offer several advantages, including low sensitivity, complex mobile phases, and time-consuming extraction procedures with limited applicability the technological maturity is low in most cases and the reproducibility of device performance is limited. Many of the reported experiments still need to be evaluated with complex instrumentation and toxic reagents for the pretreatments. A summary of the results obtained in this study compared with previously reported works is presented in Table 1 (ref. 27–33) showing that the developed method has certain advantages over previous approaches in terms of stability, suitable surface area, and feasible biological activity. Notably, our study's strengths include the utilization of a calorimetric chemosensing procedure to detect sotalol in blood samples for the first time.

Our approach represents a reliable colorimetric method for the quantitative analysis of sotalol in human real samples. Concerning its response, the suggested chemosensor approach surpasses the performance of methods reported previously. Compared to previously reported findings (Table 1), the results achieved in this study demonstrate that the developed method offers several advantages over previous approaches, such as enhanced stability, suitable surface area, and feasible biological activity. Many of the reported experiments still need to be evaluated with complex instrumentation and toxic reagents for the pretreatments. Compared to previous results (Table 1), the results obtained in this study show that the developed method offers several advantages over previous approaches, such as improved stability, a suitable surface area and realizable biological activity. The strengths of our study include, in particular, that for the first time, a calorimetric chemosensing method was used to detect sotalol in blood samples. We believe that the

Table 1 The analytical performances of various methods for the identification of sotalol

Detection method	Nano probe, nanoparticle	Liner range	LOD/LOQ/LLOD/LLOQ	Ref.
Electrochemical sensor	$NiFe_2O_4$–MWCNTs	0.5–1000 μmol L^{-1}	0.09 μmol L^{-1}	27
	Quantum dots (GQD-SH) and gold nanoparticles (AuNPs)	0.1–250 μM	0.035 μM	28
Surface-enhanced Raman scattering (SERS)	Ag@SiO_2 NPs	10^{-5} to 10^{-8} mol L^{-1}	10^{-9} mol L^{-1}	29
Electrochemical sensor	Ag/AgCl	0.39–4.22 μmol L^{-1}	0.031 μmol L^{-1}	30
	Tetrazolium blue (TB)/gold nanoparticles (GNPs)-modified carbon paste electrodes	1.0×10^{-7}–7.5×10^{-4} M	2.5×10^{-8} M	31
HPLC-MS/MS method	Gene ABCB1	0.46, 0.8 ng mL^{-1}	0.8 ng mL	32
High-performance liquid chromatography with UV detection (HPLC/UV)	—	0.05–100 μg m^{-1}	0.01 and 0.04 μg mL^{-1}	33
Colorimetric and spectrophotometric	AgNPs	0.001–20 mM	1 μM (LLOQ)	This work

proposed approach represents a reliable bioassay for the quantitative analysis of sotalol in real samples. In terms of response, the proposed chemosensor approach outperforms previous methods.

The constructed colorimetric platform was also utilized to detect spiked sotalol in plasma samples by AgNPs stabilized on a glass vial and PMMA plate (Fig. S6†). Based on the results acquired from the comparison test, different concentrations (0.001 to 20 mM) of spiked sotalol in the human plasma sample were mixed with AgNPs 1 : 0.5 : 0.5 v/v/v ratio. Then they were analyzed by colorimetric CMYK methods. According to the obtained results, the concentrations lower than 2 mM could not change the color of the mixture and in the PMMA plate, concentrations lower than 2 mM could not change the color of the mixture (Fig. S6(A1, A2 and B1, B2), and Video ESI), see ESI.†

The human plasma sample was first combined with acetonitrile in a 1 : 0.5 : 0.5 v/v/v ratio and then centrifuged for 10 min to collect the supernatant. Subsequently, it underwent analysis following the addition of various concentrations of sotalol (ranging from to 0.001 to 20 mM, at a 1 : 0.5 : 0.5 v/v/v ratio of analyte/optical probe/plasma). The positive analysis indicated no discernible variance across the different sotalol levels. However, a CMYK analysis uncovered an unexpected relationship between the sotalol concentration and absorbance, deviating from the anticipated sotalol standard concentration. The calibration curve depicted in (Fig. S6(C and D), see ESI†) illustrates the peak intensity's correlation with sotalol concentration in human plasma, ranging from 1 μM to 20 mM for 30 min incubation time. The increase in *Y* (yellow hue) value leads to a decrease in the absorbtion and the graphs of colorimetric data related to the effect of the human plasma concentration on the PMMA plate, which is an innovative initiative in this research, compared to the glass vial (Tables S1–S6†).

To assess the selectivity of the proposed colorimetric method for detection of sotalol, a mixture of AgNPs/sotalol and an inhibitory agent (in a 1 : 0.5 : 0.5 v/v/v ratio) was applied to each of the sensing zones. Initially, the PCD's sensing zones were loaded with AgNPs, AgNPs/sotalol/famotidine, AgNPs/AgNPs/sotalol/indomethacin, AgNPs/sotalol/diazepam, AgNPs/sotalol/uric acid, AgNPs/sotalol/ibuprofen, AgNPs/sotalol/bilirubin, AgNPs/sotalol (1 M)/codeine, AgNPs/sotalol/pantoprazole. To assess the selectivity of the new technique for detecting sotalol, a mixture of AgNPs/sotalol and an inhibitory agent (in a 1 : 0.5 : 0.5 v/v/v ratio) was applied to each of the sensing zones in vial and PF substrate and PMMA Plate (Fig. S7 and ESI Video†), and were observed after 30 min incubation time. According to the obtained results, the method for sotalol determination was enhanced by combining smartphone-assisted image capture and analysis by CMYK model methodology, offering advantages such as speed, low cost, reduced reagent consumption, and minimal waste generation. Replicating the digital imaging-based process is crucial to ensure accurate data analysis, as the cylindrical, hand-made box with LEDs captures images without introducing shadows or excessive brightness. The information generated during this process is dependable not only for calibration but also for determining sample composition.

The complete color change to bright pink after 30 min of reaction was just obtained for the of the (interferences/sotalol)/AgNPs mixtures had changed to a brighter pink. As adding an interference species halved the concentration of sotalol, it could be reasonable that the color of the AgNPs had not changed in other mixtures.

The interfering species with highly active functional groups could not affect the identification process of this analyte, so the pink color related to the interaction of the analyte with the optical probe remained stable and almost unchanged. The results show that the method has a wide range of applicability and only requires simple adjustments in dye dilution. Varying the number of samples will not lead to errors in the measured sotalol content. The absence of significant differences demonstrates the reliability and robustness of the following procedures (Fig. S6, see ESI†).

In summary, the colorimetric sensor addresses key limitations of existing sotalol detection methods by offering a portable, cost-effective, and user-friendly solution for real-time monitoring. This innovation has significant implications for personalized medicine, enabling healthcare providers to adjust sotalol dosages based on individual patient needs. Additionally, the platform's modular design can be adapted to detect other drugs by simply modifying the functionalization strategy.

4. Conclusion

A simple, highly sensitive assay using a high-throughput microwell array platform is presented for monitoring of sotalol as commonly applied drug in antiarrhythmic therapy. In this innovative study, the use of (AgNPs)/for optical chemosensing of sotalol was investigated. The analytical results obtained for the proposed AgNPs-based colorimetric chemosensor were comparable to other reports, as this colorimetric system has a suitable linearity range of 0.001–20 mM and possesses a reasonable LLOQ of 1 μM. Alos, two novel PCDs have been developed for portable and one-drop analysis of sotalol in human plasma samples. Using colorimetric platform, sotalol was quantified in microliter volume in 5 min of reaction time with AgNPs. So, a rapid strategy was suggested for the sensitive and selective determination of the β-blockers in real samples using the digital image analysis method. The experimental results have shown that the model-based tool achieves more accurate results than the color deconvolution and CMYK model for naked-eye sensing of sotalol. We have also illustrated that the proposed model has a little variation between data sets for PF and PMMA microplates and provides a method for estimating the concentration of analyte based on color changing. This study presents a new method for measuring sotalol using a simple and rapid portable device. Finally, we proved that quantitative colorimetric sensing of sotalol is possible based on a novel flexible substrate (PF) and polymeric microplates (PMMA). The proposed opto-sensor responds to the key limitations of existing sotalol detection methods and provides a cost-effective solution for the continuous monitoring of sotalol concentration levels. This innovation has significant

implications for personalizing treatment/medicine and enables healthcare providers to adjust sotalol doses based on individual patient conditions.

Data availability

Access to the data used in this study is available upon request and may be subject to approval by the data provider. Restrictions may apply to the availability of these data, which were used under license for this study. Interested parties are encouraged to contact the corresponding author for further information on accessing the data. All relevant data supporting the findings of this study are available within the article and its ESI files,† or from the corresponding author upon reasonable request. Access to some data may be restricted due to privacy or ethical restrictions. Any restrictions to data availability will be disclosed at the time of data request.

Conflicts of interest

There are no conflicts to declare.

Acknowledgements

We are grateful for financial assistance for this work from the Tabriz University of Medical Sciences' Pharmaceutical Analysis Research Center (Tabriz, Iran). (Grant No. 76255).

References

1 J. Larson, L. Rich, A. Deshmukh, E. C. Judge and J. J. Liang, *J. Clin. Med.*, 2022, **11**, 3233.
2 Y. Yang, Y. Wang, Z. Bao, Q. Yang, Z. Zhang and Q. Ren, *Molecules*, 2021, **26**, 468.
3 J. Liu, H. Zhang, L. Ai, X. Wei and J. Wang, *J. Food Compos. Anal.*, 2024, **133**, 106340.
4 A. Chmangui, M. Safta, M. R. Driss, S. Touil and S. Bouabdallah, *J. Chromatogr. Sci.*, 2024, **62**, 686–695.
5 N. A. Aldawsari, H. M. AlBishri, B. H. Alshammari and D. A. El-Hady, *J. Anal. Chem.*, 2024, **79**, 1808–1817.
6 S. Yıldırım and H. E. Sellitepe, *J. Chromatogr. A*, 2021, **1642**, 462007.
7 K. Sobczak, K. Rudnicki and L. Poltorak, *Analyst*, 2024, **149**, 2363–2373.
8 A. Bathinapatla, S. Kanchi, R. Chokkareddy, R. P. Puthalapattu and M. R. Kumar, *Microchem. J.*, 2023, **192**, 108930.
9 M. Liu, R. Xiao, B. Feng, D. Fan, S. Huang, A. Bi, S. Zhong, X. Feng, S. Liu and W. Zeng, *Sens. Actuators, B*, 2021, **342**, 130038.
10 M. Liu, X. Yu, M. Li, N. Liao, A. Bi, Y. Jiang, S. Liu, Z. Gong and W. Zeng, *RSC Adv.*, 2018, **8**, 12573–12587.
11 M. Liu, S. Zhong, B. Feng, Y. Ren, X. Liu, S. Bai, F. Chen, S. Liu and W. Zeng, *Chin. Chem. Lett.*, 2023, **34**, 107940.
12 R. García-Azuma, K. Werner, C. Revilla-Monsalve, O. Trinidad, N. F. Altamirano-Bustamante and M. M. Altamirano-Bustamante, *Front. Bioeng. Biotechnol.*, 2024, **12**, 1421831.
13 Z. Li, R. Zhang, X. Lu, L. Hu, X. Wang, W. Liu, C. Cui and X. Liu, *Anal. Chem.*, 2021, **93**, 13990–13997.
14 S. Soares, G. M. Fernandes and F. R. Rocha, *TrAC, Trends Anal. Chem.*, 2023, 117284.
15 Y. Li, X. Zhang, L. Yang, R. Zhang and R. Li, *Text. Res. J.*, 2023, **93**, 2718–2737.
16 K. A. Santoso, A. Kamsyakawuni and S. V. R. Izza, *J. Comput. Digital Bus.*, 2024, **3**, 112–120.
17 T. Cigula, T. Hudika and D. Donevski, *Color Res. Appl.*, 2022, **47**, 172–181.
18 Y. Zhang, P. Wang, W. Wei and Z. Wang, *Buildings*, 2024, **14**, 2874.
19 Y.-T. Lin and G. D. Finlayson, *Sensors*, 2021, **21**, 5586.
20 F. Bahavarnia, H. N. Baghban, M. Eskandani and M. Hasanzadeh, *RSC Adv.*, 2023, **13**, 30499–30510.
21 F. Bahavarnia, F. Kohansal and M. Hasanzadeh, *RSC Adv.*, 2024, **14**, 2610–2620.
22 A. Mobed, F. Kohansal, S. Dolati and M. Hasanzadeh, *RSC Adv.*, 2023, **13**, 30925–30936.
23 H. K. Kordasht, A. Saadati and M. Hasanzadeh, *Food Chem.*, 2022, **373**, 131411.
24 F. Bahavarnia and M. Hasanzadeh, *J. Photochem. Photobiol., A*, 2025, 116335.
25 I. Oshina and J. Spigulis, *J. Biomed. Opt.*, 2021, **26**, 100901.
26 M. Muthumanjula and R. Bhoopalan, *J. IoT Social, Mobile, Anal. Cloud*, 2022, **4**, 54–72.
27 A. A. Ensafi, A. R. Allafchian, B. Rezaei and R. Mohammadzadeh, *Mater. Sci. Eng., C*, 2013, **33**, 202–208.
28 M. Roushani, Z. Jalilian and A. Nezhadali, *Heliyon*, 2019, **5**(6), e01984.
29 T. Cheng, Z. Xie, T. Wang, Y. Jiang, X. Guo, X. Liu, Y. Wen, H. Yang and Y. Wu, *Anal. Chem.*, 2024, **96**, 16379–16386.
30 G. Fix, B. Coldibeli and E. R. Sartori, *Electroanalysis*, 2024, **36**, e202300419.
31 M. A. Mohamed, A. M. Fekry, M. A. El-Shal and C. E. Banks, *Electroanalysis*, 2017, **29**, 2551–2558.
32 N. Starodubtseva, S. Kindysheva, A. Potapova, E. Kukaev, Z. Khodzhaeva, E. Bockeria, V. Chagovets, V. Frankevich and G. Sukhikh, *Int. J. Mol. Sci.*, 2023, **24**, 1848.
33 S. Ansari and M. Karimi, *Med. Chem. Res.*, 2017, **26**, 2477–2490.